Scientific Research Publishing

Materials Sciences and Applications, 2024, 15, 504-527
https://www.scirp.org/journal/msa
ISSN Online: 2153-1188
ISSN Print: 2153-117X

Dental Post Based on Epoxy Resin/ Zirconium Phosphate Composite Aiming Prosthetic Dentistry

Bruna Maria De Carvalho Martins[1], Enzo Erbisti Garcia[1], Gerson Alberto Valencia Albitres[1], Daniela De França Da Silva Freitas[1], Eduardo Moreira Da Silva[2], João Luiz Portella Duarte[3], Luis Claudio Mendes[1*]

[1]Institute of Macromolecules Professor Eloisa Mano, Federal University of Rio de Janeiro, Rio de Janeiro, Brazil
[2]School of Dentistry, Federal Fluminense University, Niterói, Brazil
[3]Faculty of Odontology, State University of Rio de Janeiro, Rio de Janeiro, Brazil
Email: brunamariacm@hotmail.com, enzoerbisti@ima.ufrj.br, gvalenciaa@ima.ufrj.br, danielafranca@ima.ufrj.br, em_silva@id.uff.br, joaoduarte1000@gmail.com, *lcmendes@ima.ufrj.br

How to cite this paper: Martins, B.M.C., Garcia, E.E., Albitres, G.A.V., Freitas, D.F.S., Silva, E.M., Duarte, J.L.P. and Mendes, L.C. (2024) Dental Post Based on Epoxy Resin/ Zirconium Phosphate Composite Aiming Prosthetic Dentistry. *Materials Sciences and Applications*, **15**, 504-527.
https://doi.org/10.4236/msa.2024.1511034

Received: October 6, 2024
Accepted: November 15, 2024
Published: November 18, 2024

Abstract

The aim of this research was to develop an intrarradicular dental post based on epoxy resin/nano zirconium phosphate composite with potential application in prosthetic dentistry. Zirconium phosphate (ZrP) nanoparticle was synthesized by a reaction between phosphoric acid (H_3PO_4) and zirconium (IV) oxide chloride 8-hydrate ($ZrOCl_2{\cdot}8H_2O$) and applied as filler. Commercial epoxy resin and hardener were used as polymer matrix. The composites were prepared at different proportions of epoxy resin/hardener, filler amount, reaction time and temperature. Infrared revealed that degree of conversion decreased with amount of ZrP. Insoluble matter was upper than 97%. Thermogravimetry indicated two steps of degradation. The best values of flexural modulus and flexural strength were achieved for the post designated as 1:0.25:0.25. Laser scanning confocal microscopy suggested that the morphology of the posts fractured surface varied according to epoxy-resin:hardener ratio and the ZrP amount. From atomic force microscopy, the topographic view exposed the shape and size of ZrP particles. Field emission scanning electron microscopy and energy dispersive spectroscopy indicated good adhesion between epoxy resin matrix-ZrP and that the presence of phosphate rendered brittle the fracture surface.

Keywords

Epoxy Resin, Zirconium Phosphate, Flexural Properties, Fracture Surface, Adhesion

1. Introduction

Intraradicular posts are used in dentistry for the rehabilitation of teeth that have suffered significant loss of coronal structure, usually due to deep caries, fractures, or trauma, and following endodontic treatment, which removes the dental pulp and can compromise the strength of the tooth. The rehabilitation with fiberglass posts has been widely discussed in the literature [1] emphasizing that fiberglass posts have an elastic modulus similar to the dentin, promoting better distribution of masticatory forces and reducing the risk of fractures. According to Meriç *et al.*, glass fibers reinforced composites improve the mechanical properties of polymers and are additionally considered biocompatible and non-cytotoxic materials [2]. The better choice between metal or fiber posts remains in dentistry. Both types offer advantages and disadvantages. In the clinical context, fracture resistance and preservation of remaining tooth structure must be considered. Due to their high elastic modulus, metal posts offer high strength but concentrate greater stress on the remaining tooth structure, potentially leading to irreparable root fractures while fiber posts present the elastic modulus closer to the dentin promoting better stress distribution, and then reducing the risk of catastrophic failures [3]-[6] emphasized the biomimetic behavior of fiberglass posts, underlining the importance of mimicking dentin elasticity as a strategy to prevent root fractures. Comparisons are not restricted to their mechanical behavior. The aesthetics approach is very important in the dental field. Metal posts show critical issues related to the aesthetics and corrosion resistance. When the aesthetics are priority, fiberglass posts are preferred due to their translucency and harmomious integration with ceramic restorations [7] [8]. There are studies in which the selection between customized quartz posts, fiberglass posts, or anatomized posts should be based on the specific characteristics of each clinical case. Zavanelli *et al.* emphasized that customizing quartz posts with composite resin is essential for optimizing adaptation to the root canal and then is an effective solution for ensuring proper retention, especially for irregular canals [9]. In dental research, it has been disseminated that prefabricated posts are not suitable for widespread use. They pointed out that the application of computer aided design-computer aided manufacturing (CAD-CAM) are powerful tools to develop customized posts. They provided better adaptation to different canal shapes, ensuring stable and long-lasting retention, force distribution beyond aesthetic appeal [10]-[12]. Through CAD-CAM technology, Kasuya *et al.* mixed of diglycidildimethacrylate of bisphenol A (BisGMA) and triethylene glycol dimethacrylate (TEGDMA) reinforced with short 3-mm glass fiber and silanated $BaAlSiO_2$ viewing to develop a composite as customized posts [13]. The authors stated that the posts revealed great biomechanical behavior with the improvement of high fracture load and stress distribution. Ceramic posts are also considered in rehabilitations. According to Ramos Júnior *et al.* ceramic posts fabricated with the aid of CAD-CAM has demonstrated advantages in root canal adaptation and aesthetics if compared to traditional prefabricated posts [14]. In micro and nanoscale, epoxy resin has been applied as polymer matrix for micro and nanocomposites.

When incorporated with inorganic fillers high performance materials can be achieved. Azizi and Eslami-Farsani built composites based on epoxy resin embedded with basalt fibers and zirconia nanoparticles (ZrO_2) [15]. The samples were compounded with 100:15 (epoxy resin:hardener ratio) plus 50 wt.% of basalt fibers and ZrO_2 (1 - 5 wt.%). The composite with 3 wt.% of ZrO_2 indicated increase in the flexural strength and modulus of 90% and 74%, respectively. Aiming the preparation of prototype for endodontic implant, Widodo *et al.* synthesized fillers of ZrO_2, SiO_2 and mixing of them which were embedded in poly(methyl methacrylate) (PMMA) matrix. Three types of silane coupling agents were used. The authors stated that sample SiO_2/ZrO_2/TMSPMA presented flexural strength, diametrical tensile strength and elastic modulus of 152.7 ± 13.0 MPa, 51.2 ± 0.6 MPa, and 9272.8 ± 2481.4 MPa, respectively. These values were considered close to the dentin mechanical properties [16]. Baghdadi *et al.* modified zinc oxide (ZnO) with dopamine and two types of silanes [17]. The modified fillers was inserted into epoxy resin matrix. It was noticed the enhancement of the resin fracture toughness (around 9%) using ZnO functionalized. Focusing dental field, Soares *et al.* investigated the influence of surface treatment on the mechanical properties of carbon and glass fibers posts [18]. The authors concluded that abrasion of fiber-reinforced posts significantly affected the mechanical properties of fiber posts and their adhesion with resin cement. Among thermosetting polymers, epoxy resin is widely studied in academia and in the industrial areas. Due to its highlighted chemical, thermal and mechanical properties finds applications as surface coating, adhesives, electronic and thermal devices, and so on [19] [20]. Since the 1950s, layered phosphates have been extensively studied. With the advent of nanotechnology, layered zirconium and titanium phosphates are the most widely disseminated in the scientific literature. Their outstanding properties address their applicability in different sectors such as fuel cell membranes, catalysis, ions exchange, fire retardant, microbiology and so many others [21]-[25]. Herein, the bibliographic search did not reveal any studies related to the study of dental posts containing nano zirconium phosphate. In this context, the aim of this research was to develop an intraradicular dental post based on epoxy resin incorporated with nano zirconium phosphate, aiming for the possibility of application in prosthetic dentistry.

2. Materials and Methods

2.1. Materials

The materials utilized in this study included phosphoric acid (85%), zirconium (IV) oxide chloride 8-hydrate ($ZrOCl_2{\cdot}8H_2O$), absolute ethanol was obtained from Sigma-Aldrich. Commercial epoxy resin (Bisphenol A-epichlorohydrin prepolymer CAS 25068-38-6-3 units of bisphenol-A, molar mass 853 g/mol) and the hardener (cycloaliphatic amine) were purchase from Siligel. For mould construction, commercial silicon resin and hardener were bought from Siligel. All reagents were used as received.

2.2. Zirconium Phosphate (ZrP) Synthesis

Nano-zirconium phosphate (ZrP) was synthesized using P:Zr ratio equal 18; a mixture of phosphoric acid (H_3PO_4) and zirconium (IV) oxide chloride 8-hydrate ($ZrOCl_2{\cdot}8H_2O$) was kept under reflux, for 48 hours; sequentially, the precipitated was centrifuged, washed with distilled water until pH of 6. Finally, the product was dried in an oven, at 80˚C, until constant weight [26].

2.3. Composite Preparation

Mixing of epoxy resin and hardener at different mass ratios (1:0.25; 1:0.5 and 1:1 wt./wt.%) was used as obtain polymer matrix. Zirconium phosphate (ZrP) nanoparticle was applied as filler at different wt.% (0; 0.25; 0.5 and 1) related to resin:hardner weight ratio. To accommodate the post, a mould was prepared by mixing of silicon resin + hardener (1:0.05 wt./wt.%) as specified in the label. The composites were prepared at different weight ratios of resin/hardener, filler amount, reaction time and temperature as shown in Table 1. To better understand, the steps of the mould construction as well as the prepared pin were highlighted (Figure 1).

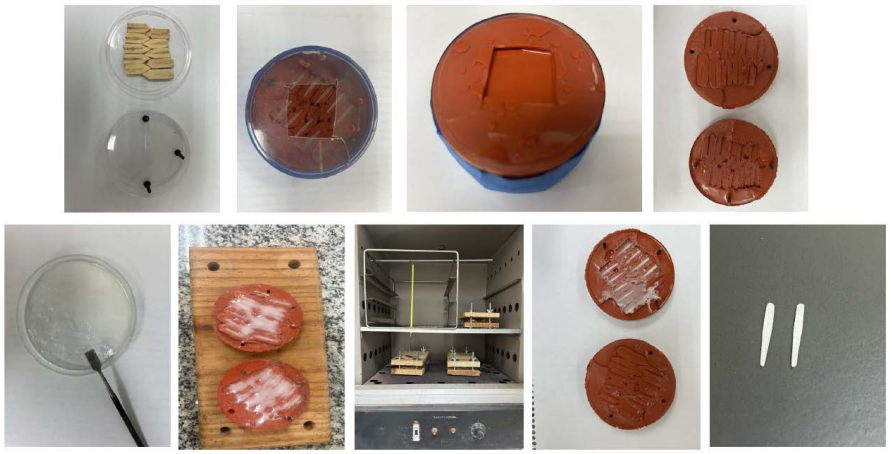

Figure 1. Representation of the steps of mould construction and post preparation.

Table 1. Samples' specifications.

Group	Resin + Hardener*	ZrP*	Temperature (˚C)	Time (h)
I	1:0.25	0	70	4
	1:0.25	0.25	70	4
	1:0.25	0.5	70	4
II	1:0.5	0	70	4
	1:0.5	0.25	70	4
	1:0.5	0.5	70	4
III	1:1	0	70	4
	1:1	0.25	70	4
	1:1	0.5	70	4

Continued

IV	1:0.5	0	70	24
	1:0.5	0.5	70	24
V	1:0.5	0	90	4
	1:0.5	0.5	90	4

*Weight ratio.

2.4. Wide Angle X-Ray Diffractometry (WAXD)

Diffraction analysis was carried out in a Rigaku Ultima IV diffractometer using 40 kV, 20 mA, step of 0.05, 2θ angle ranging from 2˚ to 40˚.

2.5. Fourier Transform Infrared Spectroscopy (FTIR)

The infrared evaluation was performed in Perkin-Elmer equipment, model Frontier MIR/FIR, within the range of 4000 - 400 cm^{-1}. The spectra were obtained by attenuated total reflectance (ATR), using 60 scans and a resolution of 4 cm^{-1}. Before and after curing, the epoxy resin degree of conversion was evaluated by ratio between absorptions at 914 cm^{-1} (epoxy ring group, variable band) and 1581 cm^{-1} (C=C aromatic ring, invariable band). Each ratio value was divided by the same ratio determined using the uncured resin. The difference from 100% was considered the degree of conversion [27] [28].

2.6. Insoluble Content

The insoluble content was determined by immersing the specimen in the absolute ethanol. Two specimens were taken in ethanol for 24 hours. After that, the specimens were removed from the liquid and left in an oven for 24 hours. The specimen weight was weighted before and after its immersion in the liquid. The weight difference was taken and related to the initial specimen weight and accepted as extracted matter. The insoluble matter was calculated considering the initial mass of the specimen as 100% and decreasing the value of the extracted.

2.7. Thermogravimetric Analysis (TGA)

TGA data was acquired throughout TA analyzer model Q500, between 30˚C - 700˚C, at 10˚C·min^{-1}, under a nitrogen atmosphere. T_{onset}, T_{max} and the temperatures where the mass loss were 10, 25, 50, 75 wt.%—T_{10}, T_{25}, T_{50}, T_{75}—were registered.

2.8. Flexural Properties

The flexural properties were performed adapting the ISO 4049 Standard in an Emic DL2000, load cell 20 kN, speed of 1 mm/min. Seven specimens were tested being the flexural modulus and flexural strength evaluated. The median was considered. The fractured surface was evaluated to the confocal and AFM equipments.

2.9. Laser Scanning Confocal Microscopy (LSCM)

The analysis was conducted in OLS4100 Olympus equipment in the specimens after the flexural test. Images of the transversal surface topograph were taken when possible.

2.10. Atomic Force Microscopy (AFM)

AFM analysis was conducted in Park Systems XE7 equipment. For each sample, a disk with 2 mm was prepared, cutting it through Isomet machine and polished with sandpapers with different grain sizes.

2.11. Field Emission Scanning Electron Microscopy and Energy Dispersive Spectroscopy (FESEM/EDS)

The transverse section SEM images were captured using a Tescan field emission microscope, model MIRA 4 LMU (LowVac Mode UniVac^{TM}) equipment, voltage of 10 kV). Elemental analysis was performed with an EDS detector equipped with a 30 mm^2 Si_3N_4 window, with a resolution lower than 129 eV for the MnKα emission line.

3. Results and Discussion

3.1. Wide Angle X-Ray Diffractometry (WAXD)

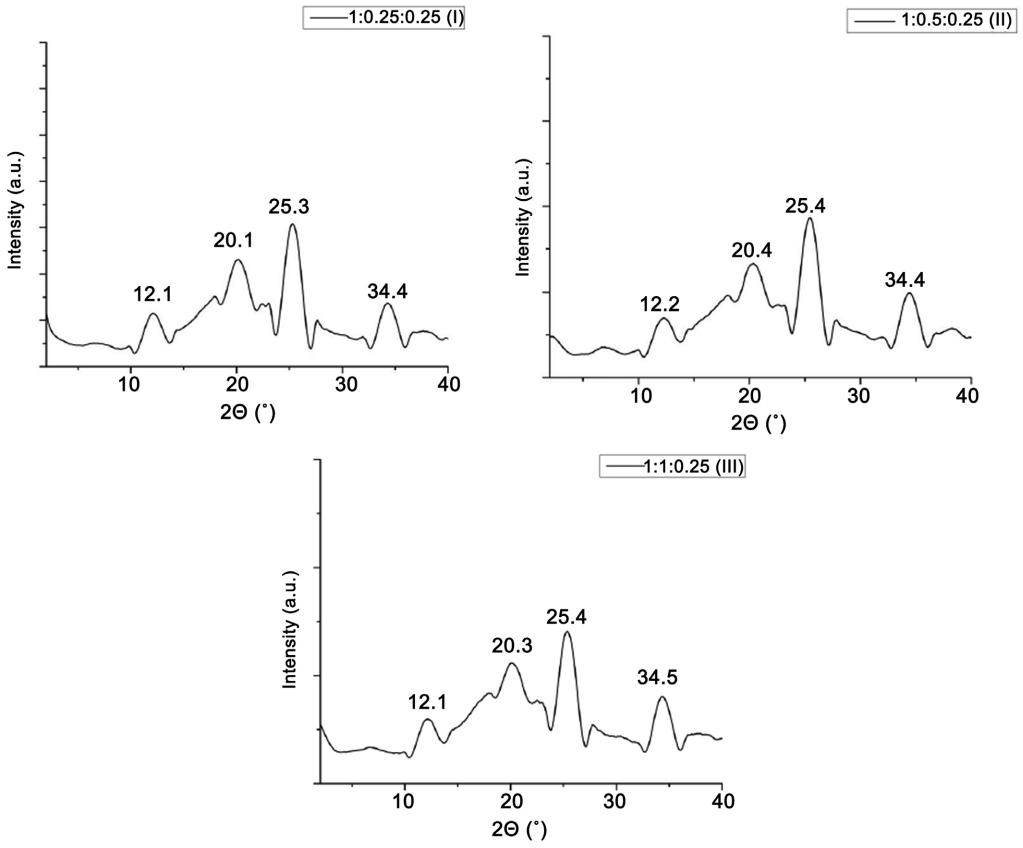

Figure 2. Representative posts' X-ray diffraction patterns (I, II and III Denote Group).

All samples revealed very similar X-ray diffraction patterns. For this analysis, the posts contained 0.25 wt.% of ZrP were chosen as representative varying the ratio of epoxy resin:hardener 1:0.25, 1:0.50 and 1:1 (**Figure 2**). Diffraction angles were recorded at 12.1˚, 20.1˚, 25.3˚ and 34.4˚ which correspond to the ZrP crystallographic planes d_{002}, d_{110}, d_{112} and d_{009}, respectively [29] [30]. As amorphous polymer, the epoxy resin did not exhibit crystalline planes.

3.2. Fourier Transform Infrared Spectroscopy (FTIR)

Due to their similarity, **Figure 3** displays the representative posts' infrared spectra of each Group. The absorptions at 3393 cm^{-1} (N-H stretching); 2958 cm^{-1} (C-H stretching of CH_3); 2914 cm^{-1} (C-H stretching of CH_2), 2870 cm^{-1} (C-H stretching of aldehyde); 1607 cm^{-1} (N-H bending); 1581 cm^{-1} (C=C aromatic ring); 1454 cm^{-1} (CH_2 deformation mode) 1362 cm^{-1} (C-O stretching); 1295 cm^{-1} (C-C-H aromatic ring); 1181 cm^{-1} (C-O and C-N deformation mode); 1034, 1018 and 961 cm^{-1} (P-O-H and PO deformation mode); 914 cm^{-1} (epoxide ring vibration); 828 cm^{-1} (C-O-O epoxy ether and C-H out of plane deformation mode) were endorsed with the articles of Sabu *et al.*, Sukanto *et al.*, Ullah *et al.* and Mendes *et al.* [27] [28] [31] [32]. **Table 2** presents the epoxy resin degree of conversion arranged according to the ratio of epoxy resin:hardener as function of ZrP content, time and temperature. The pins without ZrP showed a high degree of conversion (70-80%). Increasing reaction time and temperature, the degree of conversion was not affected. The addition of ZrP showed significant influence on the degree of conversion. Posts of the Group II and III showed a significant decrease in the degree of conversion. The greatest decrease was observed in the posts of the Group III (0.5 wt.% of ZrP). When the time reaction was increased there was an

Table 2. Posts' degree of conversion.

Resin + Hardener*	ZrP*	Degree of conversion (%)
1:0.25	0	74
1:0.5	0	74
1:1	0	80
1:0.5	0	81**
1:0.5	0	73***
1:0.25	0.25	43
1:0.5	0.25	44
1:1	0.25	53
1:0.25	0.5	---#
1:0.5	0.5	29
1:1	0.5	9
1:0.5	0.5	39**
1:0.5	0.5	27***

*Weight ratio; **24 h; ***90˚C; #no post formation.

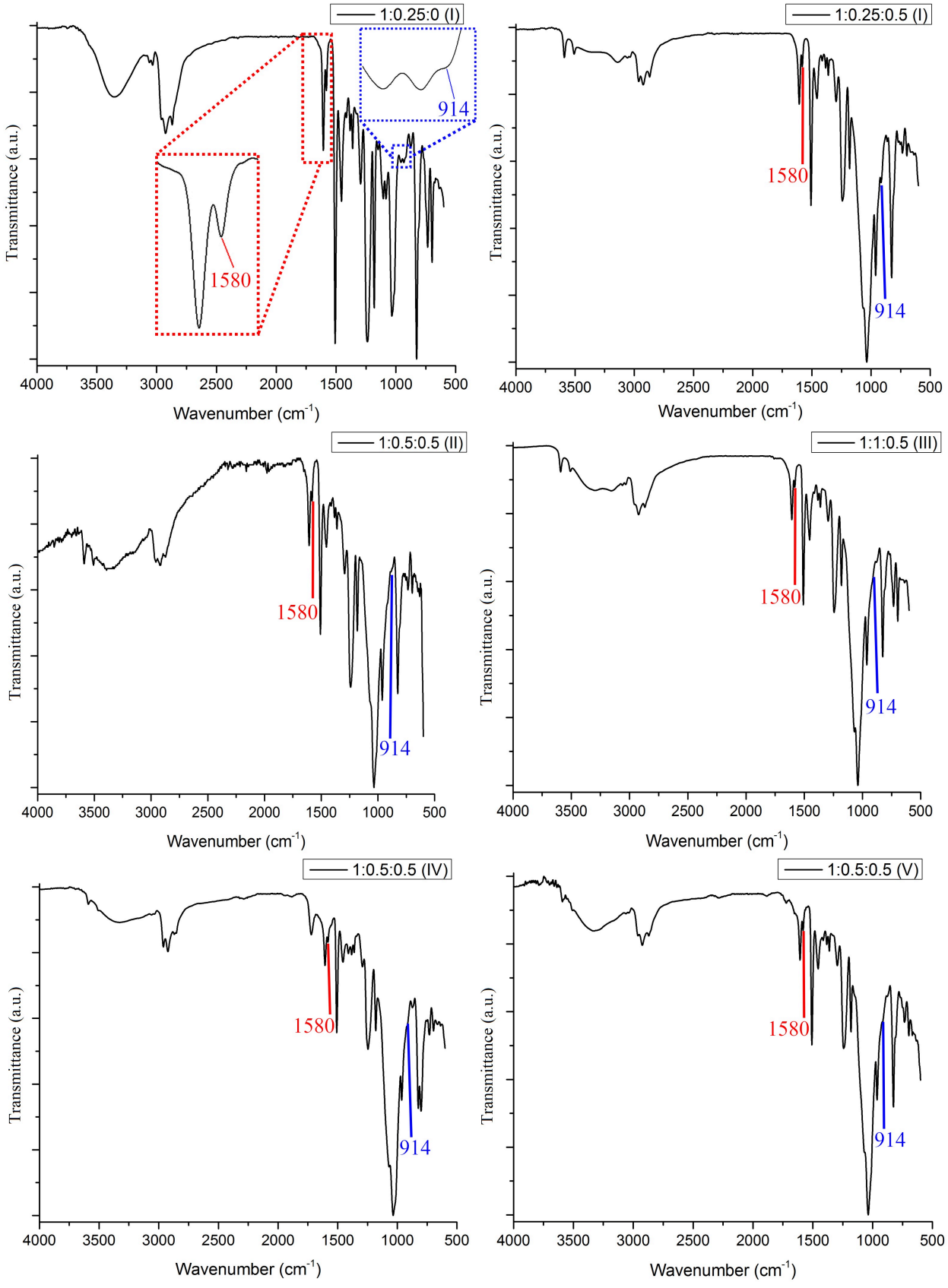

Figure 3. Representative infrared spectra of the posts (I, II, III, IV and V Denote Group).

increment of 34% in the degree of conversion (1:0.5:0.5, Group) while the increase of the reaction temperature did not reveal any improvement. The variation of the posts' degree of conversion with the addition of ZrP can be attributed to the restriction of mobility of the reactive groups of the epoxy resin and the hardener. The phosphate structure promoted a type of physical block, reducing the chances of collision between the epoxide groups and the amine groups, which resulted in a lower degree of conversion.

3.3. Insoluble Content

To evaluate the effect of epoxy resin:hardener ratio on the insoluble matter, the posts contained 0.25 wt.% of ZrP were chosen with ratios of 1:0.25, 1:0.50 and 1:1. As seen in Table 3, the insoluble content ranged between 97% - 99%. It was understood that the time and temperarure used in the posts' preparation were enough to maintain the molecules of epoxy resin and hardener in an interconnected network independent on the degree of conversion attained for each one. The behavior coud be extended to the posts embedded with 0.5 wt.% of ZrP.

Table 3. Posts' insoluble content.

Group	Epoxy resin + Hardener*	ZrP*	Insoluble matter (%)
I	1:0.25	0.25	99
II	1:0.5	0.25	98
III	1:1	0.25	97

*Weight ratio.

3.4. Thermogravimetry (TGA)

Figure 4 shows the loss mass and derivative curves of the posts 1:0.25:0, 1:0.25:0.5, 1:0.5:0.5, 1:1:0.5, 1:0.5:0.5, 1:0.5:0.5 (Groups are described in parentheses). All samples revealed two steps of degradation. In general, the first one occurred around 100˚C - 300˚C while the second one appeared at 300˚C - 500˚C. Table 4 displays the maximum degradation temperature and onset temperature of each post. T_{onset} of the posts ranged from 320˚C to 340˚C. The values found for the posts obtained at 24 hours and 90˚C were slightly upper than those build at 4 hours and 70˚C. Similar behavior was observed for T_{max1} and T_{max2}. Zhang *et al.* developed composites based on epoxy resin containing ZrP viewing application as flame retardant. The presence of the phosphate decreased the thermal stability. Only one step of degradation was detected and T_{max} varied between 370˚C - 380˚C [33]. Guo *et al.* prepared a composite of epoxy resin compounded with mixing of aluminum oxide/aluminum oxide modified with magnetite ($Al_2O_3/Al_2O_3@Fe_3O_4$) [20]. Only one degradation step was found and there was no improvement in the thermal stability. The two degradation steps may be related to the reaction conditions (time and temperature) that were not enough to promote complete curing of the resin. Regardless of the presence of filler, all posts showed two steps of thermal

degradation. From insoluble content, it was possible supposed that even with incomplete curing, there is a three-dimensional network formed by the reaction between epoxy and amine groups meaning that practically there were not free molecules of resin and hardener into the posts. Thus, the two degradation steps represent domains with unven crosslinking density.

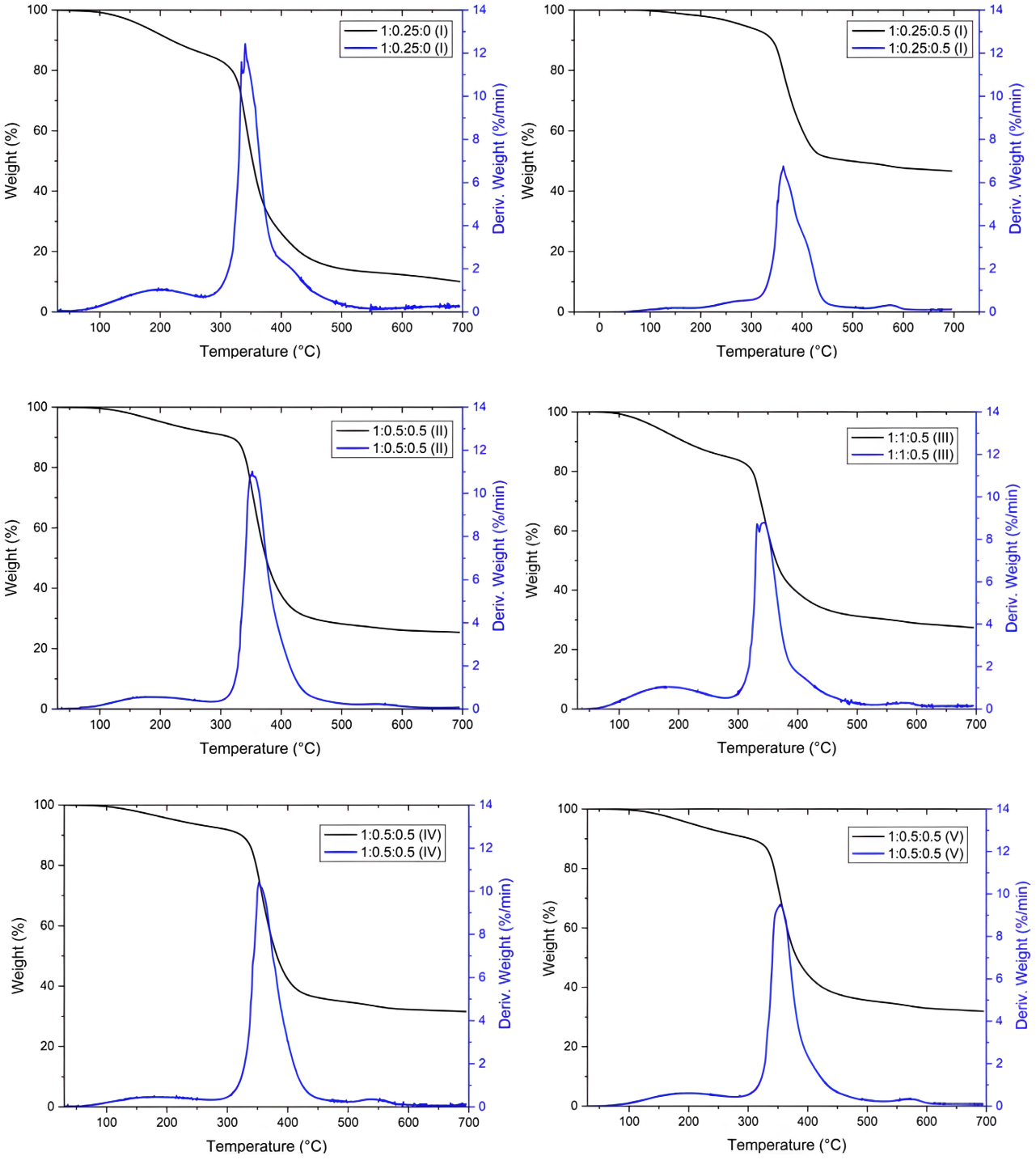

Figure 4. TG/DTG curves of the posts (I, II, III, IV and V Denote Group).

Table 4. Samples' thermogravimetry data.

Group	Sample	1st degradation interval (˚C)	T_{max1} (˚C)	2nd degradation interval (˚C)	T_{max2} (˚C)	T_{onset} (˚C)
I	1:0.25:0	100 - 300	197	300 - 500	340	325
	1:0.25:0.25	100 - 300	187	300 - 500	335	323
	1:0.25:0.5	---*	---*	---*	---*	---*
II	1:0.5:0	150 - 300	240	300 - 500	343	334
	1:0.5:0.25	100 - 300	180	300 - 500	337	327
	1:0.5:0.5	100 - 300	176	300 - 500	352	336
III	1:1:0	100 - 300	161	300 - 500	341	324
	1:1:0.25	100 - 300	178	300 - 500	335	326
	1:1:0.5	100 - 300	178	300 - 500	342	324
IV	1:0.5:0	150 - 300	226	300 - 500	350	340
	1:0.5:0.5	100 - 300	180	300 - 500	352	337
V	1:0.5:0	100 - 300	239	300 - 500	352	340
	1:0.5:0.5	100 - 300	202	300 - 500	353	334

*No post formation.

3.5. Flexural Properties

Figures 5(a)-(e) shows the representative curves of the flexural test. For the posts of the Group I, that one without ZrP (1:0.25:0) the mechanical profile seemed to be a hard and soft material. Regions of yielding, cold drawing and breaking. The curve of the post (1:0.25:0.25) presented britlle behavior. For the Group II, the post without ZrP had similar mechanical mode to that Group I without breaking. The posts (1:0.5:0.25) and (1:0.5:0.5) broken as a brittle material. For the posts of the Group III, the curves with and without ZrP resembled a plasticizing material without yielding region. All of them did not break. For the posts of the Group IV and V, the mechanical behavior of the posts (1:0.5:0) and (1:0.5:0.5) were resembled to their counterparts in Group II. Table 5 displays the flexural modulus and strength. The results did not show trend. For the posts of Group I, the presence of ZrP in the post (1:0.25:0.25) induced an increase of 54% and 18% of the flexural modulus and flexural strength, respectively. Group II registered an increment of the flexural modulus (4.9 %) for the post (1:0.5:0.5) but the flexural strength of (1:0.5:0.25) and (1:0.5:0.5) posts were significantly decreased. For all posts of the Group III, flexural modulus and strength attained the worst values. When time (Group IV) and temperature (Group V) were increased no improvement of the mechanical properties was noticed. The flexural properties of six commercial endodontic fiber posts were evaluated by Plotino and collaborators. The flexural modulus ranged from 24.4 ± 3.8 GPa and 108.6 ± 10.7 GPa for silica fiber and stainless posts, respectively. The flexural strength fluctuated from 879.1 ± 66.2 MPa and 1545.3 ± 135.9 MPa for silica fiber and cast gold fiber posts, respectively.

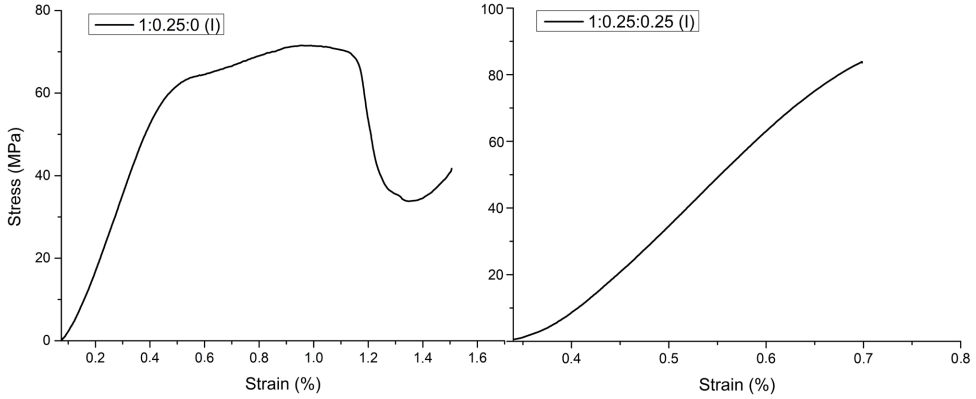
1:0.25:0 (I)
1:0.25:0.25 (I)
Stress (MPa)
Strain (%)
Strain (%)

(a)

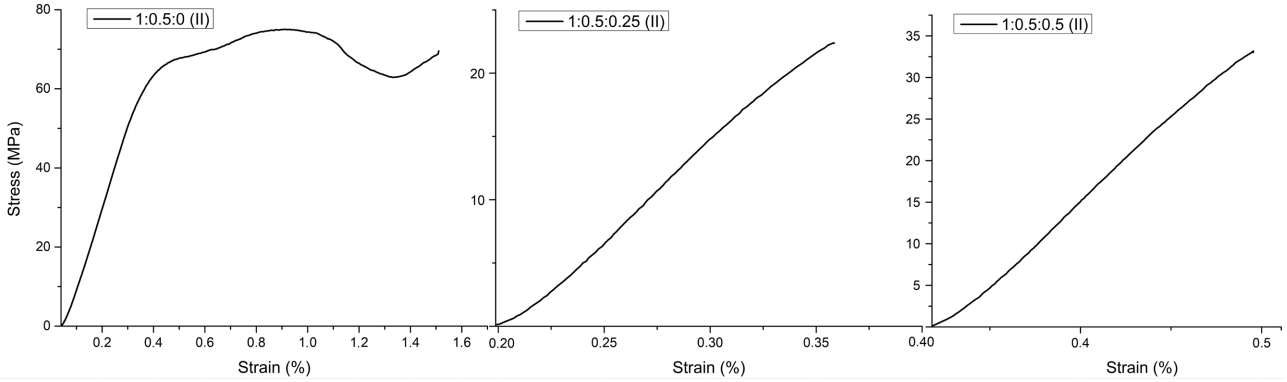
1:0.5:0 (II)
1:0.5:0.25 (II)
1:0.5:0.5 (II)
Stress (MPa)
Strain (%)
Strain (%)
Strain (%)

(b)

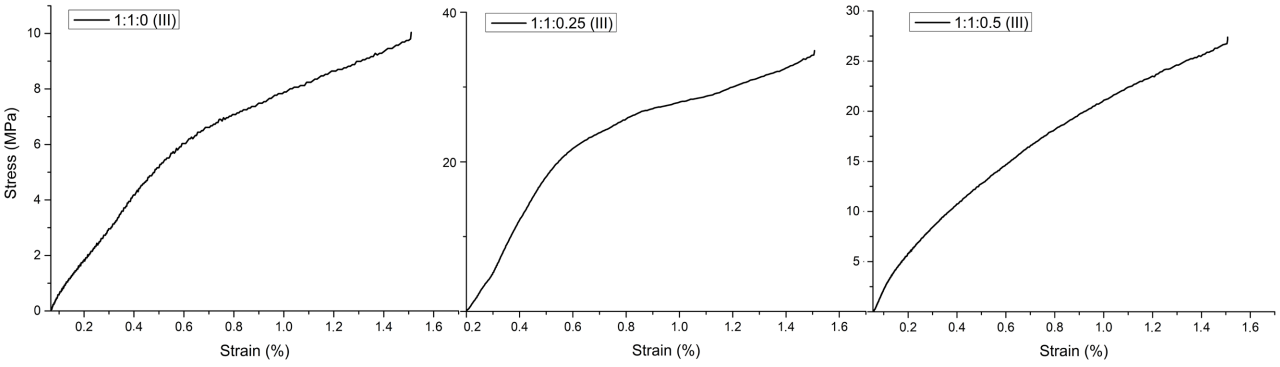
1:1:0 (III)
1:1:0.25 (III)
1:1:0.5 (III)
Stress (MPa)
Strain (%)
Strain (%)
Strain (%)

(c)

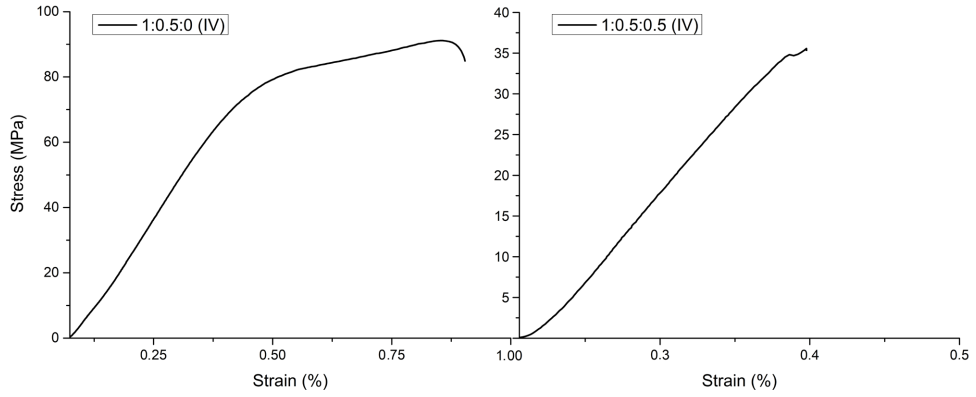
1:0.5:0 (IV)
1:0.5:0.5 (IV)
Stress (MPa)
Strain (%)
Strain (%)

(d)

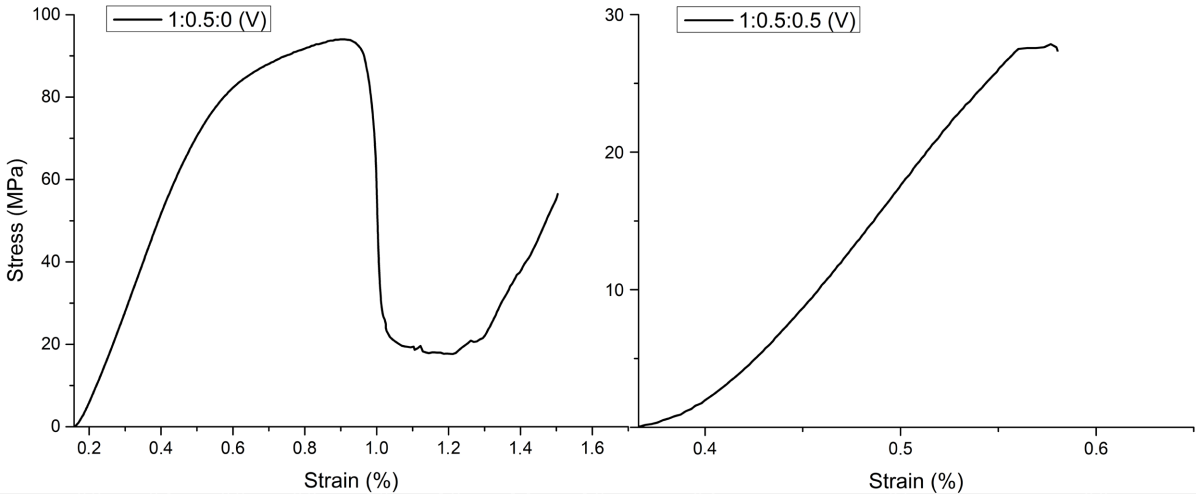

(e)

Figure 5. (a) Flexural stress-strain curves (Group I); (b) Flexural stress-strain curve (Group II); (c) Flexural stress-strain curve (Group III); (d) Flexural stress-strain curve (Group IV); (e) Flexural stress-strain curve (Group V).

Table 5. Flexural modulus and strength of the posts.

Group	Epoxy resin + Hardener*	ZrP*	Flexural Modulus** (MPa)	Flexural Strength** (MPa)
I	1:0.25	0	509	71
	1:0.25	0.25	785	84
	1:0.25	0.5	---***	---***
II	1:0.5	0	577	75****
	1:0.5	0.25	576	22
	1:0.5	0.5	605	33
III	1:1	0	26	10****
	1:1	0.25	200	35****
	1:1	0.5	85	27****
IV	1:0.5	0	624	91
	1:0.5	0.5	605	35
V	1:0.5	0	645	93
	1:0.5	0.5	495	28

*Weight ratio; **median value; ***no post formation; ****no break.

The values were upper than those observed for flexural modulus and flexural strength of human dentin, 17.5 ± 3.8 GPa and 212.9 ± 41.9 MPa, respectively [34]. Taskiran *et al.* compounded a dental formulation based on composite containing mixing of monomers—ethoxylated bisphenol A glycol dimethacrylate (Bis-EMA) plus urethane dimetacrylate (UDMA) plus triethylene glycol dimethacrylate (TEGDMA) which was embedded with barium glass, colloidal and fumed silica, zirconia (ZrO_2) and hydroxyapatite (HA) nanoparticles [35]. According to the

authors, flexural strength (70 - 80 MPa) and flexural modulus (3.5 - 4.0 GPa) were superior than that for control sample. Zirconium dioxide (ZrO_2) stabilized with yttrium oxide (Y_2O_3) has been used as dental prosthetics material. Mustafa *et al.* prepared composites of ZrO_2 and Y_2O_3 (0.5 to 3.0 wt.%) in matrix of epoxy resin. The flexural strength varied between 90 - 110 MPa and for both composites the best behavior was achieved to 1 wt.% of each oxide [36]. Considering the reaction parameters—resin:hardener ratio, ZrP content, time and temperature reaction, it was possible to verify that each Group presents a specific behavior. For Groups I and II there was some improvement in the modulus independent of the resin:hardener ratio, but the increase in the hardener content causes a sharp decline in the flexural strength. The best mechanical properties were achieved for the post 1:0.25:0.25. In group III, the modulus and flexural strength were the worst while the variation of time and temperature did not produce the expected results. The poor results could be associated with the low resin degree of conversion, agglomeration of ZrP nanoparticles and also their distribution and dispersion in the epoxy resin matrix.

3.6. Laser Scanning Confocal Microscopy (LSCM)

Confocal images (**Figure 6(a)**) and three-dimensional topology (**Figure 6(b)**) of the fractured surface from flexural test of the following posts: 1:0.25:0 and 1:0.25:0.25 (Group I); 1:0.5:0.25 and 1:0.5:0.5 (Group II); 1:0.5:0 and 1:0.5:0.5 (Group IV); 1:0.5:0 and 1:0.5:0.5 (Group V) were evaluated. In **Figure 6(a)**, Group I posts surfaces presented as continuous slots which were better seen in the post without ZrP. The presence of the ZrP rendered the surface rougher. About epoxy resin-ZrP adhesion, it was believed that it was high, although some voids were noticed which could be associated with the localized poor dispersion of ZrP in the epoxy matrix. The surface images of the Group II posts showed great similarity to that one of Group I with ZrP. As can be seen, the post with the higher ZrP content showed the largest number of voids. This irregularity could be attributed to a lower dispersibility and non-homogeneity in size of the ZrP into epoxy matrix. The posts of Group IV are related to the evaluation of the reaction time effect. The surface topology of the post without ZrP was similar to that its counterpart in Group I. The post with ZrP (50 wt.%) showed heterogeneity in the size of the ZrP domains, high adhesion between of matrix-ZrP and some voids also attributed to the dispersibility of ZrP in the polymer matrix. The images of Group V posts resembled to those of Group IV. In **Figure 6(b)**, the images possess a range of color which represents variation in the height of each surface. The purple color is related to the lowest height while the highest is the red one. The images endorse the details taken from the black and white images regarding the size heterogeneity of ZrP, its dispersion and distribution in the epoxy matrix and the matrix-ZrP adhesion. Qian *et al.* studied the use of metal cations viewing the formation of passivation of coating layer [37]. Graphene oxide was modified with cerium dioxide after being incorporated into epoxy matrix. The coating was immersed in salt solution for

14 days. After that, laser scanning confocal microscope was used to evaluate the coating corrosion. The best result was attained by the sample enriched with CeO_2@rGO/EP-0.50. Nanosheets of graphene oxide (F-GO) was chemically modified with zinc oxide quantum dots (ZnO QDs) forming nanohybrid filler labeled as F-GO@ZnO QDs [38]. Nanocomposite of waterborne epoxy coating was formulated with 1 wt.% of nanohybrid filler. By laser scanning confocal microscopy, the authors pointed out that s the roughest surface was attained with F-GO@ZnO QDs nanohybrid filler. These findings are in consonance with those of flexural analysis.

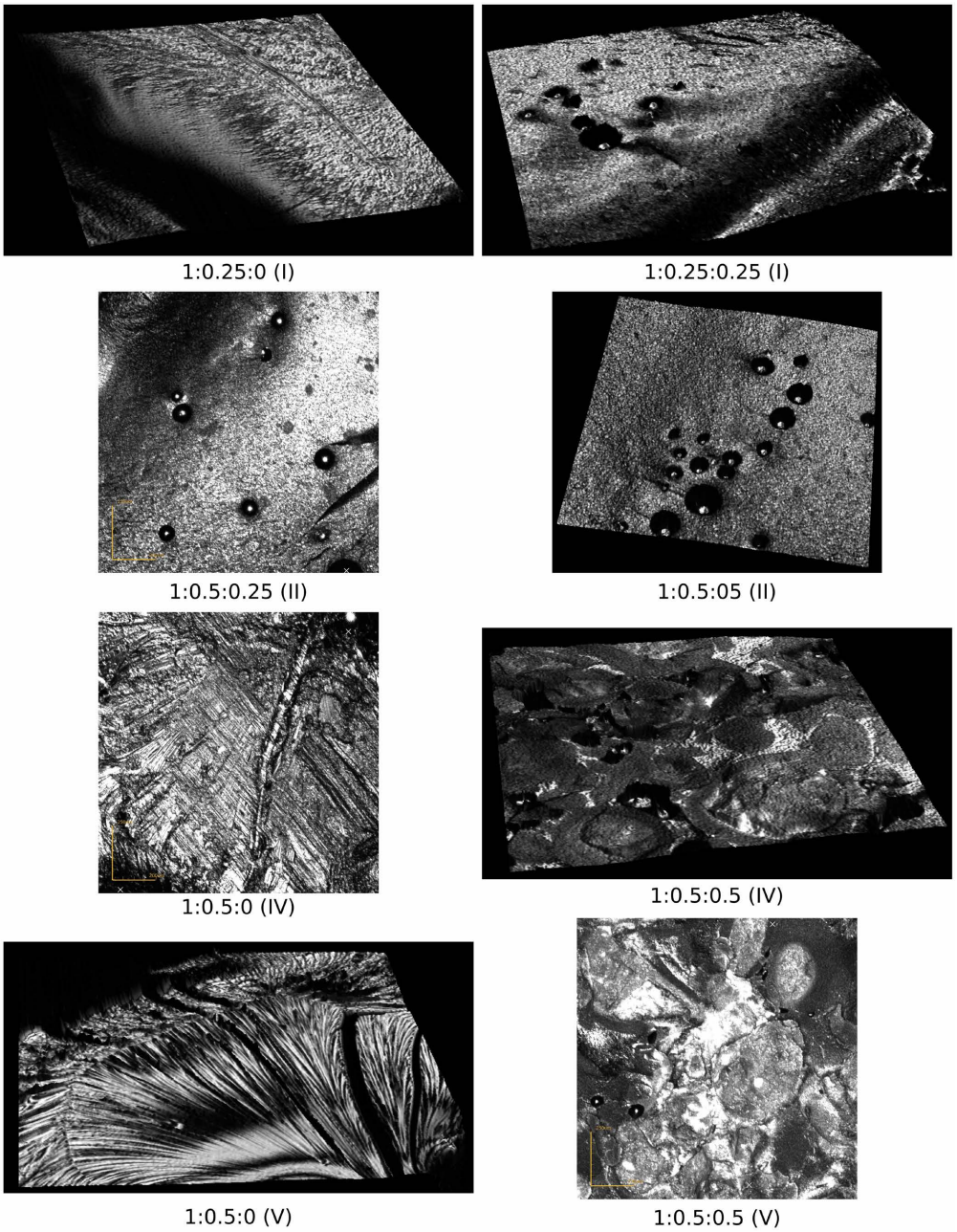

(a)

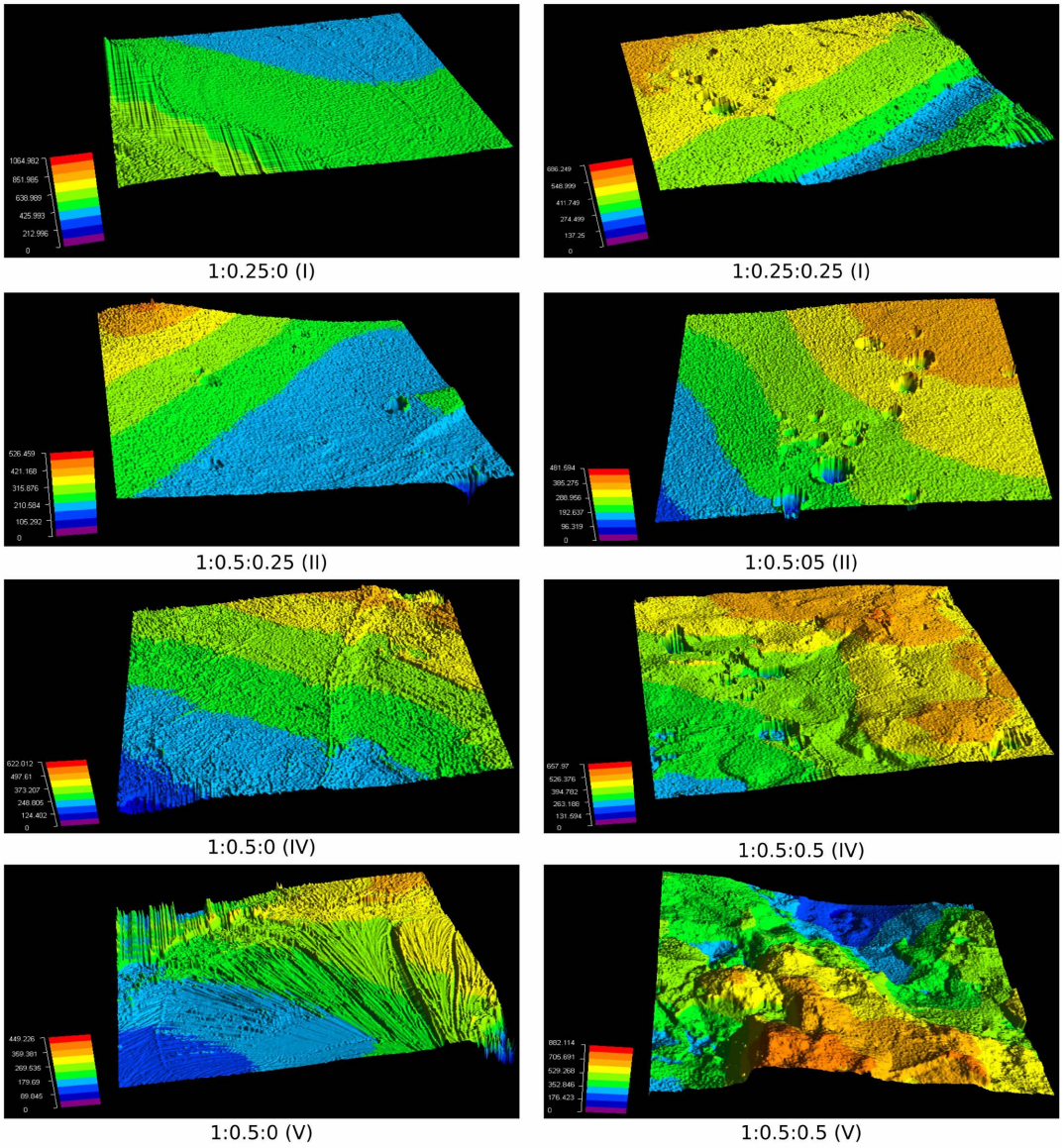

(b)

Figure 6. (a) Confocal images of the posts (I, II, IV and V Denote Group); (b) Confocal three-dimensional topology of the posts (I, II, IV and V Denote Group).

3.7. Atomic Force Microscopy (AFM)

AFM images of the 1:0.25:0.25 (Group I); 1:0.5:0.5 (Group II); 1:0.5:0.5 (Group III); 1:0.5:0.5 (Group IV); 1:0.5:0.5 (Group V) posts are presented in **Figure 7**. Observing the topology, some similarities among the posts can be highlighted such as the lamellar nature and nanometric size of ZrP, heterogeneity of size, dispersion and distribution of ZrP domains due to cluster formation. ZrP increased the posts surface roughness. Through AFM images, Khan *et al.* prepared nanocomposites based on epoxy resin embedded with alumina nanoparticles [39]. The authors associated the increase of nanocomposite breakdown strength with high surface roughness. The images showed excellent wettability of ZrP by the resin

and regardless of the conditions imposed for the development of each group of posts, it was possible to conclude that high adhesion between resin-ZrP was achieved.

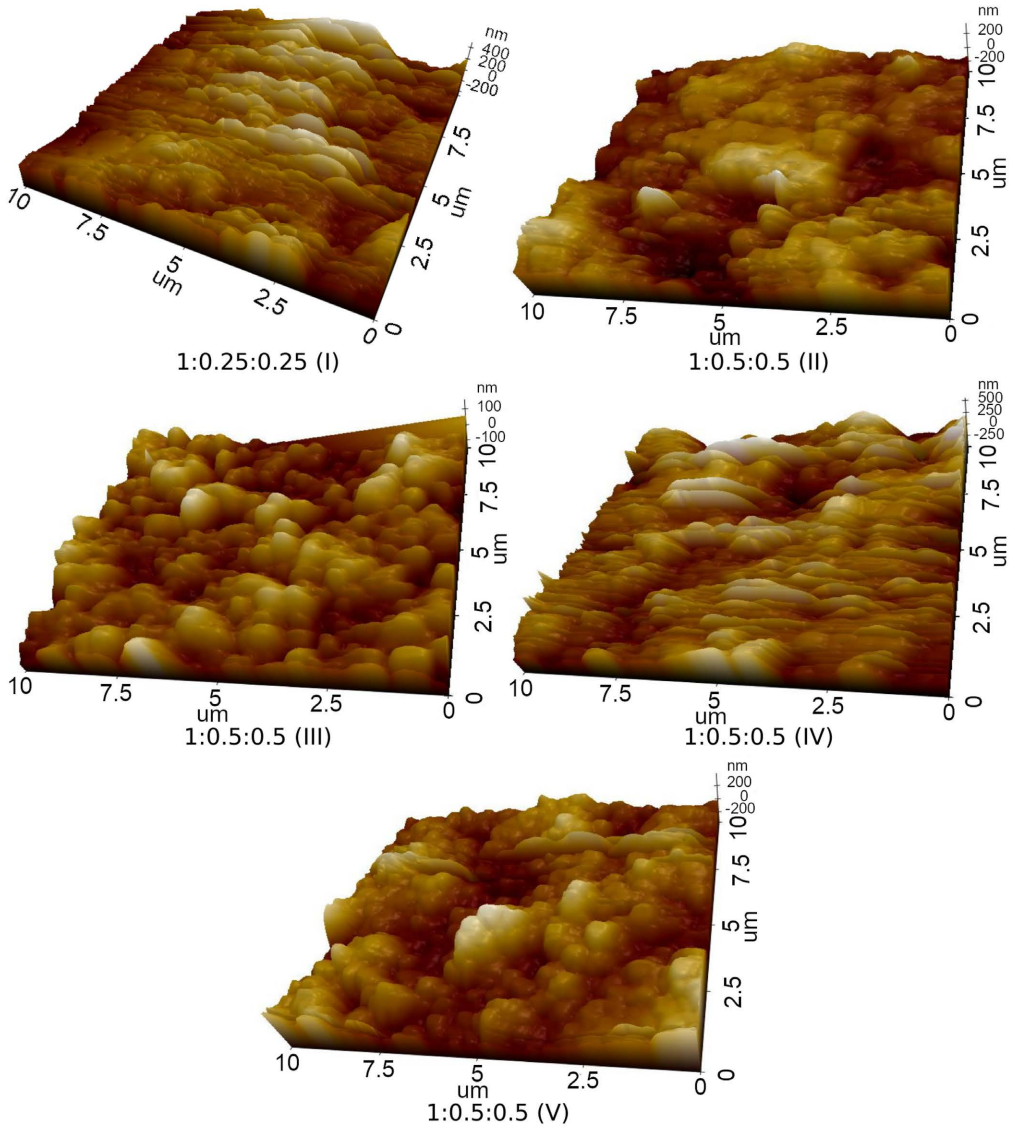

Figure 7. AFM images of the posts (I, II, III, IV and V Denote Group).

3.8. Scanning Electron Microscopy/Energy Dispersive Spectroscopy (SEM/EDS)

Figure 8 displays the SEM images of the post fractured surface of 1:0.25:0 and 1:0.25:0.25 (Group I); 1:0.5:0.25 and 1:0.5:0.5 (Group II); 1:0.5:0 and 1:0.5:0.5 (Group IV); 1:0.5:0 and 1:0.5:0.5 (Group V). Fractured surface of 1:0.25:0 post was smooth and homogeneous. High adhesion between epoxy resin-ZrP, rough surface and britle fracture were noticed for 1:0.25:0.25 post. Both posts of the Group II revealed good adhesion between epoxy resin-ZrP and good dispersion and distribution of ZrP on the epoxy resin matrix. Although there is high interconnection

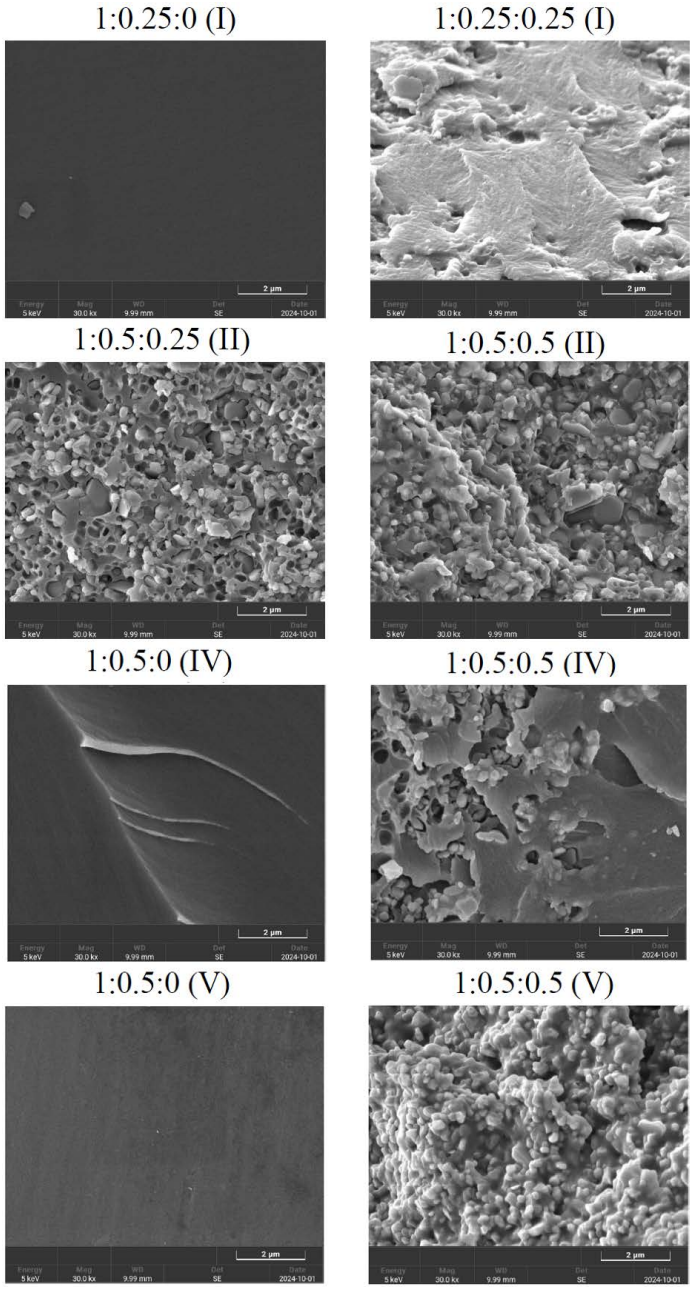

Figure 8. SEM images of posts fractured surface (I, II, IV and V Denote Group).

between epoxy resin-ZrP, a rough surface can be observed. The gray to black colored tiny regions were associated with the epoxy resin which was capable to conduct the repairation of the previous damage occurred on the fragmented surface of the ZrP particles. A brittle fracture was seen. Post formulated as 1:0.5:0 (Group IV) revealed a smooth and homogenous surface, low shearing deformation, uninterrupted crack propagation path and brittle fracture. Post designated as 1:0.5:0.5 (Group IV) showed good dispersion and distribution of ZrP, rough surface and brittle fracture. Smooth and uniform surface was noticed for the post 1:0.5:0 (Group V). The post 1:0.5:0.5 (Group V) displays high adhesion

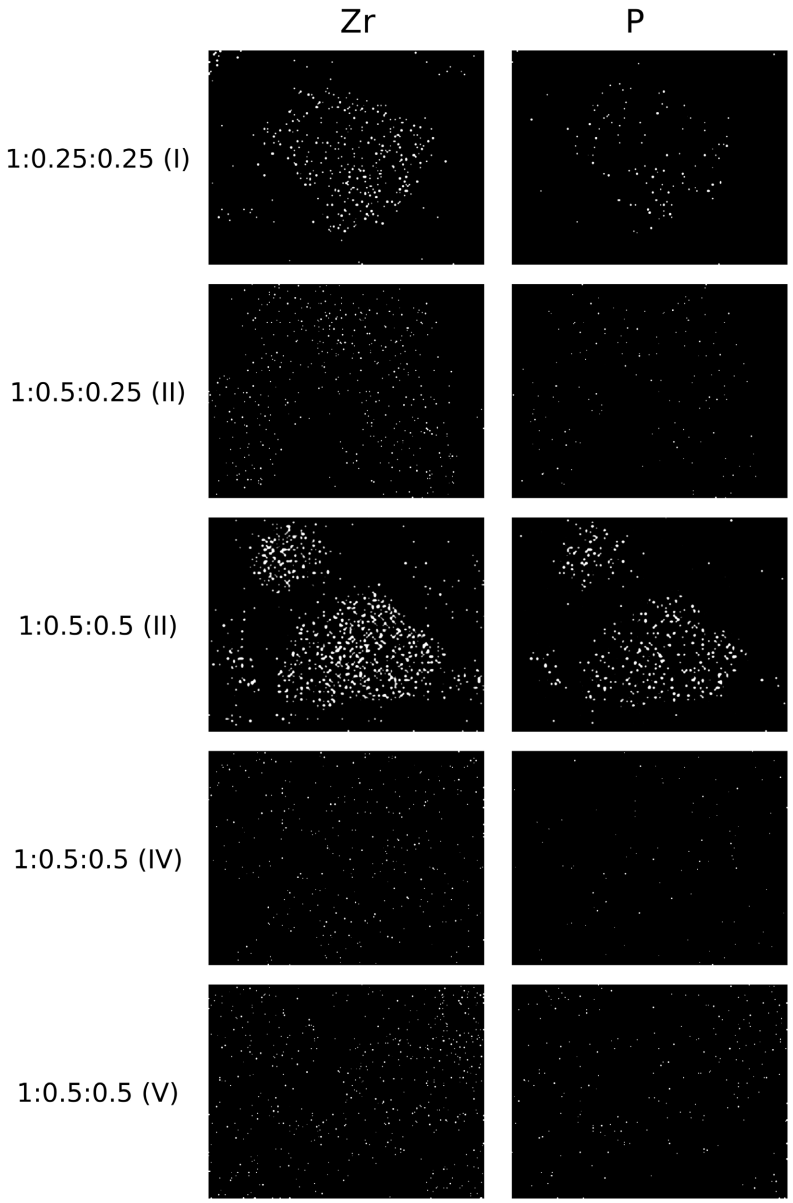

Figure 9. Dispersion and distribution of Zr and P by EDS (I, II, IV and V Denote Group).

between matrix and ZrP, good dispersion and distribution of ZrP, rough surface and brittle fracture. EDS evaluation was performed in order to describe the profle of the ZrP dispersion and distribution on the fractured surfaces (**Figure 9**). Generally speaking, the ZrP particles were better accommodated in a matrix developed from epoxy resin:ZrP ratio of 1:0.5 but their posts showed the worst mechanical results. Additionally, as the amount of ZrP increased the greatest is the roughness promoting heterogeneity in the stress distribution. Also, high content of ZrP tends to create difficulties in the collision between the reactive groups of the epoxy resin and the hardener, the degree of conversion and the crosslinking density are drastically reduced. Through dual functionalization of ZrP, Zhu *et al.* prepared exfoliated nanocomposites based on epoxy resin [40]. Although the

roughness has increased at high content of modified ZrP (16 wt.%) high elastic modulus was achieved. Composites of epoxy resin embedded with epoxy-functionalized POSS (E-POSS) and glass fiber (GF) were studied by Jiang and collaborators [41]. SEM images indicated that the epoxy resin was well accommodated in the composite with 10 wt.% of E-POSS but those ones with 10 wt.% of GF and mixing of E-POSS and GF (26 wt.%) revealed voids on account of GF pull out. Herein, the 1:0.25:0.25 post presented the best mechanical result in both modulus and flexural strength which could suggest that epoxy:resin ratio of 1:0.25 was the most suitable.

4. Conclusion

This research intended to develop composites based on epoxy resin and nano zirconium phosphate for using as intrarradicular posts. Formulations were thought by varying epoxy resin:hardener ratio, ZrP content, reaction time and temperature. When comparing the different groups of posts, the highest ZrP content was detrimental to the mechanical properties since it impaired the collision of the resin and the hardener reactive groups with an impact on the degree of conversion and crosslinking density. Epoxy resin matrix was built from a 1:0.5 ratio of epoxy resin:hardener although it has demonstrated better ZrP dispersion and distribution created posts with poor mechanical properties. Herein, the best mechanical e morphological results were attained by the post formulated as 1:0.25:0.25. The reaction time and temperature need improvement. The research continues at IMA.

Acknowledgements

The authors would like to thank the Conselho Nacional de Desenvolvimento Científico e Tecnológico (CNPq), Coordenação de Aperfeiçoamento de Pessoal de Nível Superior (CAPES) Finance Code 1, Fundação Carlos Chagas Filho de Amparo a Pesquisa do Estado do Rio de Janeiro (Faperj)—Processo E-26/200.814/2021, and Universidade Federal do Rio de Janeiro for their support of this research.

Conflicts of Interest

On behalf of all authors, the authors state that there is no conflict of interest.

Data Availability Statement

All data generated or analysed during this study are included in this published article.

References

[1] Silva, M.A.D.L., Aguiar, G.A., Boaventura, R.S.N., Santos, K.Z.S.D.S., Bastos, E.D., Adriano, G.B., *et al.* (2020) Reabilitação Estética e Funcional com Pino de Fibra de Vidro [Aesthetic and Functional Rehabilitation with Fiberglass Pin]. *Brazilian Journal of Health Review*, **3**, 17259-17267. https://doi.org/10.34119/bjhrv3n6-147

[2] Meriç, G., Dahl, J.E. and Ruyter, I.E. (2008) Cytotoxicity of Silica-Glass Fiber

Reinforced Composites. *Dental Materials*, **24**, 1201-1206. https://doi.org/10.1016/j.dental.2008.01.010

[3] Martins, M.D., Junqueira, R.B., de Carvalho, R.F., Lacerda, M.F.L.S., Faé, D.S. and Lemos, C.A.A. (2021) Is a Fiber Post Better than a Metal Post for the Restoration of Endodontically Treated Teeth? A Systematic Review and Meta-Analysis. *Journal of Dentistry*, **112**, Article ID: 103750. https://doi.org/10.1016/j.jdent.2021.103750

[4] Figueiredo, F.E.D., Martins-Filho, P.R.S. and Faria-e-Silva, A.L. (2015) Do Metal Post-Retained Restorations Result in More Root Fractures than Fiber Post-Retained Restorations? A Systematic Review and Meta-Analysis. *Journal of endodontics*, **41**, 309-316.

[5] Zhou, L. and Wang, Q. (2013) Comparison of Fracture Resistance between Cast Posts and Fiber Posts: A Meta-Analysis of Literature. *Journal of Endodontics*, **39**, 11-15. https://doi.org/10.1016/j.joen.2012.09.026

[6] Lima, D.D.S., Lima, D.C., Gomes Junior, R.D.C., Costa, K.B., Vasconcelos, O.F. and Lima, T.M.d. (2020) Comportamento biomimético dos pinos de fibra de vidro: Relato de caso. *Archives of Health Investigation*, **10**, 296-300. https://doi.org/10.21270/archi.v10i2.4880

[7] Corazza, P.H., Domênico, M.B.D., Facenda, J.C., Merlo, E.G., Borba, M. and Ozcan, M. (2022) Fiberglass versus Cast Metal Posts: A Practical Review Based on Mechanical Properties. *Brazilian Dental Science*, **25**, e3442. https://doi.org/10.4322/bds.2022.e3442

[8] Oliveira, L.K.B.F., Silva, S.R.C.D., Moura, V.S.D., Andrade, A.M.D.C., Torres, L.M.D.M., Silva, M.D.A.F.D., *et al.* (2021) Comparative Analysis between Fiberglass Post and Cast Metal Core: An Integrative Review. *Research, Society and Development*, **10**, e51610515236. https://doi.org/10.33448/rsd-v10i5.15236

[9] Zavanelli, A.C., Burlim, J.M., Silva, M.A.A., Souza, J.P.D.V. and Mazaro, J.V.Q. (2020) Pino de quartzo personalizado: Descrição da técnica e protocolo de cimentação. *Revista Odontológica de Araçatuba*, **41**, 47-52.

[10] Ruschel, G.H., Gomes, É.A., Silva-Sousa, Y.T., Pinelli, R.G.P., Sousa-Neto, M.D., Pereira, G.K.R., *et al.* (2018) Mechanical Properties and Superficial Characterization of a Milled CAD-CAM Glass Fiber Post. *Journal of the Mechanical Behavior of Biomedical Materials*, **82**, 187-192. https://doi.org/10.1016/j.jmbbm.2018.03.035

[11] Alcântara, R.Q.M. (2020) Fastening Element and System for Introduction in the Tooth Canal and Use of the Fastening Element for Introduction in the Tooth Canal. U.S. Patent Application No. 16/964, 705.

[12] Matos, L.E.F., Pacheco, E.A.M. and Guerrero, D.C.P. (2021) Intraradicular Anchor Pin ANCLA Post. US Patent Application No 10, 987, 197 B2.

[13] Barbosa Kasuya, A.V., Favarão, I.N., Machado, A.C., Rezende Spini, P.H., Soares, P.V. and Fonseca, R.B. (2020) Development of a Fiber-Reinforced Material for Fiber Posts: Evaluation of Stress Distribution, Fracture Load, and Failure Mode of Restored Roots. *The Journal of Prosthetic Dentistry*, **123**, 829-838. https://doi.org/10.1016/j.prosdent.2019.04.026

[14] Ramos Júnior, S., Felizardo, K.R., Guiraldo, R.D., Berger, S.B., Ramos, N.B.P., Assis, A.C.M.D., *et al.* (2021) CAD-CAM Endodontic Posts: Literature Review. *Research, Society and Development*, **10**, e3210111314. https://doi.org/10.33448/rsd-v10i1.11314

[15] Azizi, H. and Eslami-Farsani, R. (2019) Study of Mechanical Properties of Basalt Fibers/epoxy Composites Containing Silane-Modified Nanozirconia. *Journal of Industrial Textiles*, **51**, 649-663. https://doi.org/10.1177/1528083719887530

[16] Widodo, P., Mulyawan, W., Djustiana, N. and Joni, I.M. (2023) Synthesis and Characterization of Zirconia-Silica PMMA Nanocomposite for Endodontic Implants. *Dentistry Journal*, **11**, Article 57. https://doi.org/10.3390/dj11030057

[17] Baghdadi, Y.N., Youssef, L., Bouhadir, K., Harb, M., Mustapha, S., Patra, D., *et al.* (2020) The Effects of Modified Zinc Oxide Nanoparticles on the Mechanical/Thermal Properties of Epoxy Resin. *Journal of Applied Polymer Science*, **137**, Article ID: 49330. https://doi.org/10.1002/app.49330

[18] Soares, C.J., Santana, F.R., Pereira, J.C., Araujo, T.S. and Menezes, M.S. (2008) Influence of Airborne-Particle Abrasion on Mechanical Properties and Bond Strength of Carbon/Epoxy and Glass/Bis-GMA Fiber-Reinforced Resin Posts. *The Journal of Prosthetic Dentistry*, **99**, 444-454. https://doi.org/10.1016/s0022-3913(08)60106-7

[19] Zhang, X., Bai, T., Zhou, P., Yan, J., Yu, B., Huo, S., *et al.* (2024) Non-Phosphorus Glucosyl Schiff Bases for Smoke Inhibition and Mechanical Enhancement of Epoxy Resin Composites. *Polymer Degradation and Stability*, **223**, Article ID: 110715. https://doi.org/10.1016/j.polymdegradstab.2024.110715

[20] Guo, F., Xue, K., You, T., Hua, Z., Liu, L., Li, J., *et al.* (2024) Magnetically Assisted Construction of Al_2O_3 Platelets Dual Network and Its Excellent Thermal Conductivity in Epoxy Resin Composites. *Composites Part A*: *Applied Science and Manufacturing*, **179**, Article ID: 107988. https://doi.org/10.1016/j.compositesa.2023.107988

[21] Albitres, G., Garcia, E., Soares, C., Freitas, D., Neto, R.C. and Mendes, L. (2024) Post-consumer High Density Polyethylene/zirconium Phosphate and Aluminum Hydroxide Composites: Assessment of Physico-Mechanical and Flame Retardancy Properties. *Journal of Composite Materials*, **58**, 489-503. https://doi.org/10.1177/00219983231226278

[22] Garcia, E.E., Araujo, A.M.C.F., Albitres, G.A.V., Freitas, D.D.F.D.S., Mariano, D.M., Soares, C.M.F., *et al.* (2024) Antimicrobial Activity, Structural, Crystallographic and Thermal Characteristics of α-Titanium Phosphate Promoted by Silver Ions. *Materials Sciences and Applications*, **15**, 253-269. https://doi.org/10.4236/msa.2024.158018

[23] Kojima, S., Lee, S., Nagata, F., Kugimiya, S. and Kato, K. (2020) Protein Immobilisation onto Zirconium Phosphate with the Enhancement of the Adsorption Amount and Catalytic Activity. *Materials Today Communications*, **25**, Article ID: 101310. https://doi.org/10.1016/j.mtcomm.2020.101310

[24] Xu, L., Lei, C., Xu, R., Zhang, X. and Zhang, F. (2016) Hybridization of α-Zirconium Phosphate with Hexachlorocyclotriphosphazene and Its Application in the Flame Retardant Poly(Vinyl Alcohol) Composites. *Polymer Degradation and Stability*, **133**, 378-388. https://doi.org/10.1016/j.polymdegradstab.2016.09.025

[25] Xiao, Y., Xu, J., Huang, S. and Deng, H. (2017) Effects of α-ZrP on Crystallinity and Flame-Retardant Behaviors of PA6/MCA Composites. *International Journal of Polymer Science*, **2017**, Article ID: 6034741. https://doi.org/10.1155/2017/6034741

[26] Freitas, D.D.F.D.S., Albitres, G.A.V., Mariano, D.D.M., Cestari, S.P. and Mendes, L.C. (2022) Mechanical, Thermal, Rheological Assessment of Polyamide-6 Reinforced Composites by Addition of Lamellar Zirconium Phosphate. *Journal of Thermoplastic Composite Materials*, **36**, 2600-2622. https://doi.org/10.1177/08927057221102858

[27] Sabu, M., Bementa, E., Jaya Vinse Ruban, Y. and Ginil Mon, S. (2020) A Novel Analysis of the Dielectric Properties of Hybrid Epoxy Composites. *Advanced Composites and Hybrid Materials*, **3**, 325-335. https://doi.org/10.1007/s42114-020-00166-0

[28] Sukanto, H., Raharjo, W.W., Ariawan, D. and Triyono, J. (2023) Investigation of Cycloaliphatic Amine-Cured Bisphenol-A Epoxy Resin under Quenching Treatment

and the Effect on Its Carbon Fiber Composite Lamination Strength. *Journal of the Mechanical Behavior of Materials*, **32**, Article ID: 20220266. https://doi.org/10.1515/jmbm-2022-0266

[29] Kang, D., Yu, X., Tong, S., Ge, M., Zuo, J., Cao, C., *et al.* (2013) Performance and Mechanism of Mg/Fe Layered Double Hydroxides for Fluoride and Arsenate Removal from Aqueous Solution. *Chemical Engineering Journal*, **228**, 731-740. https://doi.org/10.1016/j.cej.2013.05.041

[30] Jiang, F., Sun, H., Chen, L., Lei, F. and Sun, D. (2019) Dispersion-tribological Property Relationship in Mineral Oils Containing 2D Layered α-Zirconium Phosphate Nanoplatelets. *Friction*, **8**, 695-707. https://doi.org/10.1007/s40544-019-0294-2

[31] Ullah, R., Ahmad, I. and Zheng, Y. (2016) Fourier Transform Infrared Spectroscopy of "Bisphenol A". *Journal of Spectroscopy*, **2016**, Article ID: 2073613. https://doi.org/10.1155/2016/2073613

[32] Mendes, L.C., Silva, D.F., Araujo, L.J.F. and Lino, A.S. (2014) Zirconium Phosphate Organically Intercalated/Exfoliated with Long Chain Amine. *Journal of Thermal Analysis and Calorimetry*, **118**, 1461-1469. https://doi.org/10.1007/s10973-014-4056-0

[33] Zhang, H., Li, K., Wang, M. and Zhang, J. (2021) The Preparation of a Composite Flame Retardant of Layered Double Hydroxides and α-Zirconium Phosphate and Its Modification for Epoxy Resin. *Materials Today Communications*, **28**, Article ID: 102711. https://doi.org/10.1016/j.mtcomm.2021.102711

[34] Plotino, G., Grande, N.M., Bedini, R., Pameijer, C.H. and Somma, F. (2007) Flexural Properties of Endodontic Posts and Human Root Dentin. *Dental Materials*, **23**, 1129-1135. https://doi.org/10.1016/j.dental.2006.06.047

[35] Tunca Taşkıran, S., Tanoğlu, M., Çerci, N., Cevahir, A., Türkdoğan Damar, C., Ünver, E., *et al.* (2024) Development of Resin-Based Dental Composites Containing Hydroxyapatite and Zirconia Nanoparticles. *Polymer Composites*, **45**, 10470-10485. https://doi.org/10.1002/pc.28488

[36] Mustafa, B.S., Jamal, G.M. and Gh. Abdullah, O. (2022) Improving the Tensile, Toughness, and Flexural Properties of Epoxy Resin Based Nanocomposites Filled with ZrO_2 and Y_2O_3 Nanoparticles. *Results in Physics*, **38**, Article ID: 105662. https://doi.org/10.1016/j.rinp.2022.105662

[37] Qian, Y., Zheng, W., Chen, W., Feng, T., Liu, T.X. and Fu, Y.Q. (2021) Enhanced Functional Properties of CeO_2 Modified Graphene/Epoxy Nanocomposite Coating through Interface Engineering. *Surface and Coatings Technology*, **409**, Article ID: 126819. https://doi.org/10.1016/j.surfcoat.2020.126819

[38] Zhou, Z., Pourhashem, S., Wang, Z., Duan, J., Zhang, R. and Hou, B. (2022) Distinctive Roles of Graphene Oxide, ZnO Quantum Dots, and Their Nanohybrids in Anti-Corrosion and Anti-Fouling Performance of Waterborne Epoxy Coatings. *Chemical Engineering Journal*, **439**, Article ID: 135765. https://doi.org/10.1016/j.cej.2022.135765

[39] khan, M.Z., Wang, F., Waleed, A., Huang, Z., Hassan, M.A.S. and Khan, A. (2020) Filler Concentration Effect on Breakdown Strength and Trap Level of Epoxy Resin-Al_2O_3 Nanocomposites. *Polymer Bulletin*, **78**, 5891-5903. https://doi.org/10.1007/s00289-020-03411-0

[40] Zhu, Z., Baker, J., Liu, C., Zhao, M., Kotaki, M. and Sue, H. (2021) High Performance Epoxy Nanocomposites Based on Dual Epoxide Modified α-Zirconium Phosphate Nanoplatelets. *Polymer*, **212**, Article ID: 123154. https://doi.org/10.1016/j.polymer.2020.123154

[41] Jiang, J., Shen, J., Yang, X., Zhao, D. and Feng, Y. (2023) Epoxy-functionalized POSS and Glass Fiber for Improving Thermal and Mechanical Properties of Epoxy Resins. *Applied Sciences*, **13**, Article 2461. https://doi.org/10.3390/app13042461